

Analyzing new physics in the decays $\bar{B}^0 \rightarrow D^{(*)}\tau^-\bar{\nu}_\tau$ with form factors obtained from the covariant quark model

M. A. Ivanov,^{1,*} J. G. Körner,^{2,†} and C. T. Tran^{1,3,4,‡}

¹ *Bogoliubov Laboratory of Theoretical Physics,
Joint Institute for Nuclear Research, 141980 Dubna, Russia*

² *PRISMA Cluster of Excellence, Institut für Physik,
Johannes Gutenberg-Universität, D-55099 Mainz, Germany*

³ *Advanced Center for Physics, Institute of Physics,
Vietnam Academy of Science and Technology, 100000 Hanoi, Vietnam*

⁴ *Department of General and Applied Physics,
Moscow Institute of Physics and Technology, 141700 Dolgoprudny, Russia*

(Dated: November 15, 2016)

Abstract

We study possible new physics (NP) effects in the exclusive decays $\bar{B}^0 \rightarrow D^{(*)}\tau^-\bar{\nu}_\tau$. We extend the Standard Model by taking into account right-handed vector (axial), left- and right-handed (pseudo)scalar, and tensor current contributions. The $\bar{B}^0 \rightarrow D^{(*)}$ transition form factors are calculated in the full kinematic q^2 range by employing a covariant quark model developed by us. We provide constraints on NP operators based on measurements of the ratios of branching fractions $R(D^{(*)}) \equiv \mathcal{B}(\bar{B}^0 \rightarrow D^{(*)}\tau^-\bar{\nu}_\tau)/\mathcal{B}(\bar{B}^0 \rightarrow D^{(*)}\mu^-\bar{\nu}_\mu)$ and consider the effects of these operators on physical observables in different NP scenarios. We also derive the fourfold angular distribution for the cascade decay $\bar{B}^0 \rightarrow D^{*+}(\rightarrow D^0\pi^+)\tau^-\bar{\nu}_\tau$ which allows one to analyze the polarization of the D^* meson in the presence of NP effects. We discuss several strategies to distinguish between various NP contributions.

*Electronic address: ivanovm@theor.jinr.ru

†Electronic address: jukoerne@uni-mainz.de

‡Electronic address: ctt@theor.jinr.ru, tranchienthang1347@gmail.com

I. INTRODUCTION

In the last few years, the semileptonic decays $\bar{B}^0 \rightarrow D^{(*)}\tau^-\bar{\nu}_\tau$ have been widely discussed in the literature as candidates for testing the Standard Model (SM) and searching for possible new physics (NP) in charged-current interactions. At B factories, the Belle and *BABAR* collaborations have been continuously updating their measurements with better precision based on electron-positron colliders. Recently, the LHCb Collaboration has also entered the game with data taken at the LHC hadron collider. The three groups have reported measurements of the ratios in Refs. [1–5]. These measurements provide the average ratios

$$R(D)|_{\text{expt}} = 0.397 \pm 0.049, \quad R(D^*)|_{\text{expt}} = 0.308 \pm 0.017, \quad (1)$$

which exceed the SM expectations [6, 7]

$$R(D)|_{\text{SM}} = 0.300 \pm 0.008, \quad R(D^*)|_{\text{SM}} = 0.252 \pm 0.003, \quad (2)$$

by 1.9σ and 3.3σ , respectively.

The excess of $R(D^{(*)})$ over SM predictions has attracted a great deal of attention in the particle physics community and has led to many theoretical studies looking for NP explanations. Some studies focus on specific NP models including two-Higgs-doublet models [8–12], the minimal supersymmetric standard model [13, 14], leptoquark models [15–20], and other extensions of the SM [21, 22]. Other studies adopt a model-independent approach, in which a general effective Hamiltonian for the $b \rightarrow c\ell\nu$ transition in the presence of NP is imposed to investigate the impact of various NP operators on different physical observables [7, 23–30]. Most of the theoretical studies rely on the heavy quark effective theory (HQET) [31, 32] to evaluate the hadronic form factors, which are expressed through a few universal functions in the heavy quark limit (HQL). In the present analysis, we employ an alternative approach to calculate the NP-induced hadronic transitions based on our covariant quark model with embedded infrared confinement [for short, covariant confined quark model (CCQM)], which has been developed in some earlier papers by us (see Ref. [33, 34] and references therein).

In a recent paper [35], we have provided a thorough study of the leptonic and semileptonic decays $B^- \rightarrow \ell^-\bar{\nu}_\ell$ and $\bar{B}^0 \rightarrow D^{(*)}\ell^-\bar{\nu}_\ell$ within the SM. We have also considered the HQL in the heavy-to-heavy transition $\bar{B}^0 \rightarrow D(D^*)$ and found agreement with the HQET predictions. In this paper we follow the authors of Refs. [7, 23, 25–28] to include NP operators in the effective Hamiltonian and investigate their effects on physical observables of

the decays $\bar{B}^0 \rightarrow D^{(*)}\ell^-\bar{\nu}_\ell$. We define a full set of form factors corresponding to SM+NP operators and calculate them by employing the CCQM. In the CCQM the transition form factors can be determined in the full range of momentum transfer, making the calculations straightforward without any extrapolation. This provides an opportunity to investigate NP operators in a self-consistent manner, and independently from the HQET. We first constrain the NP operators using experimental data, then analyze their effects on various observables including the ratios of branching fractions, the forward-backward asymmetries, and a set of polarization observables. We also derive the fourfold angular distribution for the cascade decay $\bar{B}^0 \rightarrow D^{*+}(\rightarrow D^0\pi^+)\tau^-\bar{\nu}_\tau$ to analyze the polarization of the D^* meson in the presence of NP by using the traditional helicity amplitudes. A similar study was done by the authors of Refs. [27, 28], in which the angular distribution is expressed via the transversality amplitudes. The remaining part of the paper is organized as follows. In Sec. II we set up our framework by introducing the effective Hamiltonian. In this section we also describe in some detail the calculation technique used in our approach in order to derive the $\bar{B}^0 \rightarrow D^{(*)}$ transition form factors. In Sec. III we use the helicity technique to derive the twofold distribution and provide experimental constraints on the NP operators. In Sec. IV we define various physical observables obtained from the fourfold distribution and analyze their sensitivity to different NP operators. And finally, we provide a brief summary of our main results in Sec. V.

II. EFFECTIVE HAMILTONIAN AND FORM FACTORS

We start with the effective Hamiltonian for the quark-level transition $b \rightarrow c\tau^-\bar{\nu}_\tau$

$$\mathcal{H}_{eff} = 2\sqrt{2}G_F V_{cb}[(1 + V_L)\mathcal{O}_{V_L} + V_R\mathcal{O}_{V_R} + S_L\mathcal{O}_{S_L} + S_R\mathcal{O}_{S_R} + T_L\mathcal{O}_{T_L}], \quad (3)$$

where the four-Fermi operators are written as

$$\begin{aligned} \mathcal{O}_{V_L} &= (\bar{c}\gamma^\mu P_L b) (\bar{\tau}\gamma_\mu P_L \nu_\tau), \\ \mathcal{O}_{V_R} &= (\bar{c}\gamma^\mu P_R b) (\bar{\tau}\gamma_\mu P_L \nu_\tau), \\ \mathcal{O}_{S_L} &= (\bar{c}P_L b) (\bar{\tau}P_L \nu_\tau), \\ \mathcal{O}_{S_R} &= (\bar{c}P_R b) (\bar{\tau}P_L \nu_\tau), \\ \mathcal{O}_{T_L} &= (\bar{c}\sigma^{\mu\nu} P_L b) (\bar{\tau}\sigma_{\mu\nu} P_L \nu_\tau). \end{aligned} \quad (4)$$

Here, $\sigma_{\mu\nu} = i[\gamma_\mu, \gamma_\nu]/2$, $P_{L,R} = (1 \mp \gamma_5)/2$ are the left and right projection operators, and $V_{L,R}$, $S_{L,R}$, and T_L are the complex Wilson coefficients governing the NP contributions. In the SM one has $V_{L,R} = S_{L,R} = T_L = 0$. We assume that NP only affects leptons of the third generation.

The invariant matrix element of the semileptonic decays $\bar{B}^0 \rightarrow D^{(*)}\tau\bar{\nu}_\tau$ can be written as

$$\begin{aligned} \mathcal{M} = & \frac{G_F V_{cb}}{\sqrt{2}} \left[(1 + V_R + V_L) \langle D^{(*)} | \bar{c} \gamma^\mu b | \bar{B}^0 \rangle \bar{\tau} \gamma_\mu (1 - \gamma^5) \nu_\tau \right. \\ & + (V_R - V_L) \langle D^{(*)} | \bar{c} \gamma^\mu \gamma^5 b | \bar{B}^0 \rangle \bar{\tau} \gamma_\mu (1 - \gamma^5) \nu_\tau \\ & + (S_R + S_L) \langle D^{(*)} | \bar{c} b | \bar{B}^0 \rangle \bar{\tau} (1 - \gamma^5) \nu_\tau \\ & + (S_R - S_L) \langle D^{(*)} | \bar{c} \gamma^5 b | \bar{B}^0 \rangle \bar{\tau} (1 - \gamma^5) \nu_\tau \\ & \left. + T_L \langle D^{(*)} | \bar{c} \sigma^{\mu\nu} (1 - \gamma^5) b | \bar{B}^0 \rangle \bar{\tau} \sigma_{\mu\nu} (1 - \gamma^5) \nu_\tau \right]. \end{aligned} \quad (5)$$

Note that the axial and pseudoscalar hadronic currents do not contribute to the $\bar{B}^0 \rightarrow D$ transition, while the scalar hadronic current does not contribute to the $\bar{B}^0 \rightarrow D^*$ transition. Therefore, assuming that NP appears in both transitions, the cases of pure $V_R - V_L$ or $S_R \pm S_L$ couplings are ruled out, as mentioned in Ref. [23].

The hadronic matrix elements are parametrized by a set of invariant form factors as follows:

$$\begin{aligned} T_1^\mu & \equiv \langle D(p_2) | \bar{c} \gamma^\mu b | \bar{B}^0(p_1) \rangle = F_+(q^2) P^\mu + F_-(q^2) q^\mu, \\ T_2 & \equiv \langle D(p_2) | \bar{c} b | \bar{B}^0(p_1) \rangle = (m_1 + m_2) F^S(q^2), \\ T_3^{\mu\nu} & \equiv \langle D(p_2) | \bar{c} \sigma^{\mu\nu} (1 - \gamma^5) b | \bar{B}^0(p_1) \rangle = \frac{i F^T(q^2)}{m_1 + m_2} (P^\mu q^\nu - P^\nu q^\mu + i \varepsilon^{\mu\nu P q}), \end{aligned} \quad (6)$$

for the $\bar{B}^0 \rightarrow D$ transition, and

$$\begin{aligned} \epsilon_{2\alpha}^\dagger \mathcal{T}_{1L(R)}^{\mu\alpha} & \equiv \langle D^*(p_2) | \bar{c} \gamma^\mu (1 \mp \gamma^5) b | \bar{B}^0(p_1) \rangle \\ & = \frac{\epsilon_{2\alpha}^\dagger}{m_1 + m_2} (\mp g^{\mu\alpha} P q A_0(q^2) \pm P^\mu P^\alpha A_+(q^2) \pm q^\mu P^\alpha A_-(q^2) + i \varepsilon^{\mu\alpha P q} V(q^2)), \\ \epsilon_{2\alpha}^\dagger \mathcal{T}_2^\alpha & \equiv \langle D^*(p_2) | \bar{c} \gamma^5 b | \bar{B}^0(p_1) \rangle = \epsilon_{2\alpha}^\dagger P^\alpha G^S(q^2), \\ \epsilon_{2\alpha}^\dagger \mathcal{T}_3^{\mu\nu\alpha} & \equiv \langle D^*(p_2) | \bar{c} \sigma^{\mu\nu} (1 - \gamma^5) b | \bar{B}^0(p_1) \rangle \\ & = -i \epsilon_{2\alpha}^\dagger \left[(P^\mu g^{\nu\alpha} - P^\nu g^{\mu\alpha} + i \varepsilon^{P\mu\nu\alpha}) G_1^T(q^2) \right. \\ & \quad + (q^\mu g^{\nu\alpha} - q^\nu g^{\mu\alpha} + i \varepsilon^{q\mu\nu\alpha}) G_2^T(q^2) \\ & \quad \left. + (P^\mu q^\nu - P^\nu q^\mu + i \varepsilon^{Pq\mu\nu}) P^\alpha \frac{G_0^T(q^2)}{(m_1 + m_2)^2} \right], \end{aligned} \quad (7)$$

for the $\bar{B}^0 \rightarrow D^*$ transition. Here, $P = p_1 + p_2$, $q = p_1 - p_2$, and ϵ_2 is the polarization vector of the D^* meson so that $\epsilon_2^\dagger \cdot p_2 = 0$. The particles are on their mass shells: $p_1^2 = m_1^2 = m_B^2$ and $p_2^2 = m_2^2 = m_{D^{(*)}}^2$.

In Ref. [35] we have given a detailed description of the CCQM framework for the calculation of the semileptonic transitions $\bar{B}^0 \rightarrow D^{(*)}\tau^-\bar{\nu}_\tau$ in the SM. It therefore suffices to briefly describe the main steps in the corresponding calculation for a more general set of quark-level transition operators.

The CCQM provides a field-theoretic frame work for the calculation of particle transitions in the constituent quark model (see e.g., Refs. [36–41]). In the CCQM, particle transitions are calculated from Feynman diagrams involving quark loops. For example, the $\bar{B}^0 \rightarrow D^{(*)}$ transitions are described by a one-loop diagram requiring a genuine one-loop calculation. The high-energy behavior of quark loops is tempered by nonlocal Gaussian-type vertex functions with a Gaussian-type falloff behavior. The particle-quark vertices have nonlocal interpolating current structure. In the Feynman diagrams one uses the usual free local quark propagators $(m - \not{p})^{-1}$. The normalization of the particle-quark vertices is provided by the compositeness condition which embodies the correct charge normalization of the respective hadron [42]. The compositeness condition can be viewed as the field-theoretic equivalent of the normalization of the wave function of a quantum-mechanical state. A universal infrared cutoff provides for an effective confinement of quarks. There are therefore no free quark thresholds in the Feynman diagrams even if they are allowed by the kinematics of the process. We mention that the authors of Ref. [43] have pursued a related program to calculate heavy meson transitions covariantly via one-loop integrals.

The loop integrations are done with the help of the Fock-Schwinger representation of the quark propagator. The use of the Fock-Schwinger representation allows one to do tensor loop integrals in a very efficient way since one can convert loop momenta into derivatives of the exponent function which are simple to handle. We mention that the same idea to treat tensor loop integrals has been used in the evaluation of loop integrals in local quantum field theory [44, 45].

The model parameters, namely, the hadron size parameter Λ , the constituent quark masses m_{q_i} , and the universal infrared cutoff parameter λ , are determined by fitting calculated quantities of a multitude of basic processes to available experimental data or lattice simulations (for details, see Ref. [34], where a set of weak and electromagnetic decays was

used). In this paper we will use the updated least-squares fit performed in Refs. [46–48]. Those model parameters involved in this paper are given in Eq. (8) (all in GeV):

$$\begin{array}{cccccccc} m_{u/d} & m_s & m_c & m_b & \lambda & \Lambda_{D^*} & \Lambda_D & \Lambda_B \\ \hline 0.241 & 0.428 & 1.67 & 5.04 & 0.181 & 1.53 & 1.60 & 1.96 \end{array}. \quad (8)$$

Once these parameters are fixed, one can employ the CCQM as a frame-independent tool for hadronic calculation. Model-independent parameters and other physical constants are taken from Ref. [49].

The form factors in our model are represented by three-fold integrals which are calculated by using FORTRAN codes in the full kinematical momentum transfer region. Our numerical results for the form factors are well represented by a double-pole parametrization

$$F(q^2) = \frac{F(0)}{1 - as + bs^2}, \quad s = \frac{q^2}{m_1^2}. \quad (9)$$

The double-pole approximation is quite accurate: the error relative to the exact results is less than 1% over the entire q^2 range. For the $\bar{B}^0 \rightarrow D$ and $\bar{B}^0 \rightarrow D^*$ transitions the parameters of the approximation are listed in Eqs. (10) and (11), respectively:

$$\begin{array}{c|cccc} & F_+ & F_- & F^S & F^T \\ \hline F(0) & 0.79 & -0.36 & 0.80 & 0.77 \\ F(q_{\max}^2) & 1.14 & -0.53 & 0.89 & 1.11 \\ F^{HQET}(q_{\max}^2) & 1.14 & -0.54 & 0.88 & 1.14 \\ a & 0.75 & 0.77 & 0.22 & 0.76 \\ b & 0.039 & 0.046 & -0.098 & 0.043 \end{array}, \quad (10)$$

$$\begin{array}{c|ccccccccc} & A_0 & A_+ & A_- & V & G^S & G_0^T & G_1^T & G_2^T \\ \hline F(0) & 1.62 & 0.67 & -0.77 & 0.77 & -0.50 & -0.073 & 0.73 & -0.37 \\ F(q_{\max}^2) & 1.91 & 0.99 & -1.15 & 1.15 & -0.73 & -0.13 & 1.10 & -0.55 \\ F^{HQET}(q_{\max}^2) & 1.99 & 1.12 & -1.12 & 1.12 & -0.62 & 0 & 1.12 & -0.50 \\ a & 0.34 & 0.87 & 0.89 & 0.90 & 0.87 & 1.23 & 0.90 & 0.88 \\ b & -0.16 & 0.057 & 0.070 & 0.075 & 0.060 & 0.33 & 0.074 & 0.064 \end{array}. \quad (11)$$

We have also listed the zero-recoil values of our model form factors (row three) which, using the relations in Appendix A, can be compared to the corresponding HQET results (row four). The agreement between the two sets of zero-recoil values is quite good [$O(1 - 10)\%$] showing that our model calculation, which includes the full heavy mass dependence, is quite close to the heavy quark limit. It is quite noteworthy that we obtain a nonzero result for the form factor G_0^T in our model calculation at zero recoil, which is predicted to vanish in the HQL.

In Fig. 1 we present the q^2 dependence of the $\bar{B}^0 \rightarrow D^{(*)}$ transition form factors in the full momentum transfer range $0 \leq q^2 \leq q_{max}^2 = (m_{\bar{B}^0} - m_{D^{(*)}})^2$.

Finally, we briefly discuss some error estimates within our model. We fix our model parameters (the constituent quark masses, the infrared cutoff and the hadron size parameters) by minimizing the functional $\chi^2 = \sum_i \frac{(y_i^{\text{expt}} - y_i^{\text{theor}})^2}{\sigma_i^2}$ where σ_i is the experimental uncertainty. If σ is too small then we take its value of 10%. Moreover, we observed that the errors of the fitted parameters are of the order of 10%. Thus we estimate the model uncertainties within 10%.

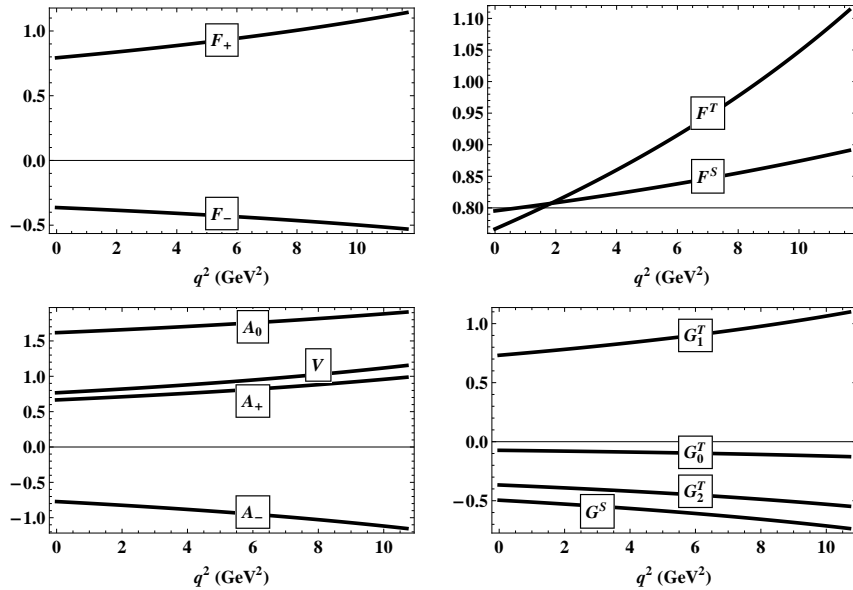


FIG. 1: Form factors of the transitions $\bar{B}^0 \rightarrow D$ (upper panels) and $\bar{B}^0 \rightarrow D^*$ (lower panels).

III. TWOFOLD DISTRIBUTION AND EXPERIMENTAL CONSTRAINTS

A. $\bar{B}^0 \rightarrow D$ transition

Using the helicity technique described in our recent paper [35] one can write the helicity amplitude of the decay $\bar{B}^0 \rightarrow D\tau^-\bar{\nu}_\tau$ as

$$\begin{aligned}
\sum_{pol} |\mathcal{M}|^2 = & \frac{G_F^2 |V_{cb}|^2}{2} \left\{ |1 + V_L + V_R|^2 \sum_{hel} H(m) H^\dagger(n) L_1(m', n') g_{mm'} g_{nn'} \right. \\
& + |S_L + S_R|^2 |H_P^S|^2 L_2 \\
& + |T_L|^2 \sum_{hel} H_T(m, n) H_T^\dagger(u, v) L_3(m', n', u', v') g_{mm'} g_{nn'} g_{uu'} g_{vv'} \\
& + (S_L + S_R)^\dagger H_P^{\dagger S} \sum_{hel} H(m) L_4(m') g_{mm'} \\
& + (S_L + S_R) H_P^S \sum_{hel} H^\dagger(m) L_5(m') g_{mm'} \\
& + T_L^\dagger \sum_{hel} H_T^\dagger(m, n) H(u) L_6(m', n', u') g_{mm'} g_{nn'} g_{uu'} \\
& \left. + T_L \sum_{hel} H_T(m, n) H^\dagger(u) L_7(m', n', u') g_{mm'} g_{nn'} g_{uu'} \right\}, \quad (12)
\end{aligned}$$

where the notation \sum_{hel} means all helicity indices appearing in the expression under the symbol are summed up. The hadronic and leptonic helicity amplitudes in Eq. (12) are defined as follows:

$$\begin{aligned}
H(m) &= \epsilon_\mu^\dagger(m) T_1^\mu, & H_P^S &= T_2, & H_T(m, n) &= i\epsilon_\mu^\dagger(m) \epsilon_\nu^\dagger(n) T_3^{\mu\nu}, \\
L_1(m, n) &= \epsilon_\mu(m) \epsilon_\alpha^\dagger(n) \text{tr}[(\not{k}_1 + m_\tau) \gamma^\mu (1 - \gamma_5) \not{k}_2 (1 + \gamma_5) \gamma^\alpha], \\
L_2 &= \text{tr}[(\not{k}_1 + m_\tau) (1 - \gamma_5) \not{k}_2 (1 + \gamma_5)], \\
L_3(m, n, r, s) &= \epsilon_\mu(m) \epsilon_\nu(n) \epsilon_\alpha^\dagger(r) \epsilon_\beta^\dagger(s) \text{tr}[(\not{k}_1 + m_\tau) \sigma^{\mu\nu} (1 - \gamma_5) \not{k}_2 (1 + \gamma_5) \sigma^{\alpha\beta}], \\
L_4(m) &= \epsilon_\mu(m) \text{tr}[(\not{k}_1 + m_\tau) \gamma^\mu (1 - \gamma_5) \not{k}_2 (1 + \gamma_5)], \\
L_5(m) &= \epsilon_\alpha^\dagger(m) \text{tr}[(\not{k}_1 + m_\tau) (1 - \gamma_5) \not{k}_2 (1 + \gamma_5) \gamma^\alpha], \\
L_6(m, n, r) &= i\epsilon_\alpha^\dagger(m) \epsilon_\beta^\dagger(n) \epsilon_\mu(r) \text{tr}[(\not{k}_1 + m_\tau) \gamma^\mu (1 - \gamma_5) \not{k}_2 (1 + \gamma_5) \sigma^{\alpha\beta}], \\
L_7(m, n, r) &= -i\epsilon_\mu(m) \epsilon_\nu(n) \epsilon_\alpha^\dagger(r) \text{tr}[(\not{k}_1 + m_\tau) \sigma^{\mu\nu} (1 - \gamma_5) \not{k}_2 (1 + \gamma_5) \gamma^\alpha].
\end{aligned}$$

One obtains the following nonzero hadronic helicity amplitudes written in terms of the invariant form factors:

$$\begin{aligned}
H_t &\equiv H(t) = \frac{1}{\sqrt{q^2}}(PqF_+ + q^2F_-), & H_0 &\equiv H(0) = \frac{2m_1|\mathbf{p}_2|}{\sqrt{q^2}}F_+, \\
H_P^S &\equiv (m_1 + m_2)F^S, \\
H_T &\equiv H_T(t, 0) = -H_T(0, t) = \pm H_T(\mp, \pm) = \frac{2m_1|\mathbf{p}_2|}{m_1 + m_2}F^T.
\end{aligned} \tag{13}$$

The differential $(q^2, \cos\theta)$ distribution is written as

$$\begin{aligned}
&\frac{d^2\Gamma(\bar{B}^0 \rightarrow D\tau^-\bar{\nu}_\tau)}{dq^2 d\cos\theta} \\
&= \frac{G_F^2|V_{cb}|^2|\mathbf{p}_2|q^2v^2}{(2\pi)^3 16m_1^2} \\
&\quad \times \left\{ |1 + V_L + V_R|^2 [|H_0|^2 \sin^2\theta + 2\delta_\tau|H_t - H_0 \cos\theta|^2] \right. \\
&\quad + |S_L + S_R|^2 |H_P^S|^2 + 16|T_L|^2 [2\delta_\tau + (1 - 2\delta_\tau) \cos^2\theta] |H_T|^2 \\
&\quad + 2\sqrt{2\delta_\tau} \text{Re}(S_L + S_R) H_P^S [H_t - H_0 \cos\theta] \\
&\quad \left. + 8\sqrt{2\delta_\tau} \text{Re}T_L [H_0 - H_t \cos\theta] H_T \right\},
\end{aligned} \tag{14}$$

where we have introduced the velocity-type parameter $v = 1 - m_\tau^2/q^2$ as well as the helicity flip factor $\delta_\tau = m_\tau^2/2q^2$. After integrating over $\cos\theta$ one has

$$\begin{aligned}
&\frac{d\Gamma(\bar{B}^0 \rightarrow D\tau^-\bar{\nu}_\tau)}{dq^2} \\
&= \frac{G_F^2|V_{cb}|^2|\mathbf{p}_2|q^2v^2}{(2\pi)^3 12m_1^2} \\
&\quad \times \left\{ |1 + V_L + V_R|^2 [(1 + \delta_\tau)|H_0|^2 + 3\delta_\tau|H_t|^2] \right. \\
&\quad + \frac{3}{2}|S_L + S_R|^2 |H_P^S|^2 + 8|T_L|^2(1 + 4\delta_\tau)|H_T|^2 \\
&\quad \left. + 3\sqrt{2\delta_\tau} \text{Re}(S_L + S_R) H_P^S H_t + 12\sqrt{2\delta_\tau} \text{Re}T_L H_0 H_T \right\}.
\end{aligned} \tag{15}$$

This q^2 distribution agrees with the result of Ref. [17]. Note that in this paper we do not consider interference terms between different NP operators.

B. $\bar{B}^0 \rightarrow D^* \tau^- \bar{\nu}_\tau$ transition

The helicity amplitude of the decay $\bar{B}^0 \rightarrow D^* \tau^- \bar{\nu}_\tau$ is written as

$$\begin{aligned}
\sum_{pol} |\mathcal{M}|^2 = & \frac{G_F^2 |V_{cb}|^2}{2} \\
& \times \left\{ \sum_{hel} \left[|1 + V_L|^2 H_L(m, r) H_L^\dagger(n, r) + |V_R|^2 H_R(m, r) H_R^\dagger(n, r) \right. \right. \\
& \left. \left. + V_R^\dagger H_L(m, r) H_R^\dagger(n, r) + V_R H_R(m, r) H_L^\dagger(n, r) \right] L_1(m', n') g_{mm'} g_{nn'} \right. \\
& + \sum_{hel} |S_R - S_L|^2 |H_V^S(r)|^2 L_2 \\
& + \sum_{hel} |T_L|^2 H_T(m, n, r) H_T^\dagger(u, v, r) L_3(m', n', u', v') g_{mm'} g_{nn'} g_{uu'} g_{vv'} \\
& + \sum_{hel} (S_R - S_L)^\dagger H_L(m, r) H_V^{S\dagger}(r) L_4(m') g_{mm'} \\
& + \sum_{hel} (S_R - S_L) H_L^\dagger(m, r) H_V^S(r) L_5(m') g_{mm'} \\
& + \sum_{hel} T_L^\dagger H_T^\dagger(m, n, r) H_L(u, r) L_6(m', n', u') g_{mm'} g_{nn'} g_{uu'} \\
& \left. + \sum_{hel} T_L H_T(m, n, r) H_L^\dagger(u, r) L_7(m', n', u') g_{mm'} g_{nn'} g_{uu'} \right\}, \tag{16}
\end{aligned}$$

where we have defined the hadronic helicity amplitudes as follows:

$$\begin{aligned}
H_L(m, r) &= \epsilon_\mu^\dagger(m) \epsilon_{2\alpha}^\dagger(r) \mathcal{T}_{1L}^{\mu\alpha}, & H_R(m, r) &= \epsilon_\mu^\dagger(m) \epsilon_{2\alpha}^\dagger(r) \mathcal{T}_{1R}^{\mu\alpha}, \\
H_T(m, n, r) &= i \epsilon_\mu^\dagger(m) \epsilon_\nu^\dagger(n) \epsilon_{2\alpha}^\dagger(r) \mathcal{T}_3^{\mu\nu\alpha}, & H_V^S(r) &= \epsilon_{2\alpha}^\dagger(r) \mathcal{T}_2^\alpha.
\end{aligned} \tag{17}$$

The nonzero helicity amplitudes read

$$\begin{aligned}
H_{00} &\equiv H_L(0, 0) = -H_R(0, 0) = \frac{-Pq(m_1^2 - m_2^2 - q^2)A_0 + 4m_1^2 |\mathbf{p}_2|^2 A_+}{2m_2 \sqrt{q^2} (m_1 + m_2)}, \\
H_{t0} &\equiv H_L(t, 0) = -H_R(t, 0) = \frac{m_1 |\mathbf{p}_2| (Pq(-A_0 + A_+) + q^2 A_-)}{m_2 \sqrt{q^2} (m_1 + m_2)}, \\
H_{\pm\pm} &\equiv H_L(\pm, \pm) = -H_R(\mp, \mp) = \frac{-PqA_0 \pm 2m_1 |\mathbf{p}_2| V}{m_1 + m_2}, \\
H_V^S &\equiv H_V^S(0) = \frac{m_1}{m_2} |\mathbf{p}_2| G^S, \\
H_T^\pm &\equiv H_T(\pm, t, \pm) = \pm H_T(\pm, 0, \pm) = -H_T(t, \pm, \pm) = \mp H_T(0, \pm, \pm) \\
&= -\frac{1}{\sqrt{q^2}} \left[(m_1^2 - m_2^2 \pm \lambda^{1/2}(m_1^2, m_2^2, q^2)) G_1^T + q^2 G_2^T \right], \\
H_T^0 &\equiv H_T(0, t, 0) = H_T(+, -, 0) = -H_T(t, 0, 0) = -H_T(-, +, 0) \\
&= -\frac{1}{2m_2} \left[(m_1^2 + 3m_2^2 - q^2) G_1^T + (m_1^2 - m_2^2 - q^2) G_2^T - \frac{\lambda(m_1^2, m_2^2, q^2)}{(m_1 + m_2)^2} G_0^T \right]. \tag{18}
\end{aligned}$$

The differential $(q^2, \cos\theta)$ distribution of the decay $\bar{B}^0 \rightarrow D^*\tau^-\bar{\nu}_\tau$ is given in Appendix C. After integrating over $\cos\theta$ one has

$$\begin{aligned}
& \frac{d\Gamma(\bar{B}^0 \rightarrow D^*\tau^-\bar{\nu}_\tau)}{dq^2} \\
&= \frac{G_F^2 |V_{cb}|^2 |\mathbf{p}_2| q^2 v^2}{(2\pi)^3 12m_1^2} \\
&\quad \times \left\{ (|1 + V_L|^2 + |V_R|^2) [(1 + \delta_\tau)(|H_{00}|^2 + |H_{++}|^2 + |H_{--}|^2) + 3\delta_\tau |H_{t0}|^2] \right. \\
&\quad - 2\text{Re}V_R [(1 + \delta_\tau)(|H_{00}|^2 + 2H_{++}H_{--}) + 3\delta_\tau |H_{t0}|^2] \\
&\quad + \frac{3}{2}|S_R - S_L|^2 |H_V^S|^2 + 3\sqrt{2\delta_\tau}\text{Re}(S_R - S_L)H_V^S H_{t0} \\
&\quad + 8|T_L|^2(1 + 4\delta_\tau)(|H_T^0|^2 + |H_T^+|^2 + |H_T^-|^2) \\
&\quad \left. - 12\sqrt{2\delta_\tau}\text{Re}T_L(H_{++}H_T^+ + H_{--}H_T^- + H_{00}H_T^0) \right\}. \tag{19}
\end{aligned}$$

This q^2 distribution agrees with the result of Ref. [17]. Note that in this paper we do not consider interference terms between different NP operators.

C. Experimental constraints

Assuming that NP only affects the tau modes, we integrate Eqs. (15) and (19) and obtain the ratios of branching fractions $R(D^{(*)})$ in the presence of NP operators. It is important to note that within the SM (without any NP operators) our model calculation yields

$$R(D) = 0.267, \quad R(D^*) = 0.238,$$

which are consistent with other SM predictions given in Refs. [6, 7, 50, 51] within 10%. In order to acquire the allowed regions for the NP Wilson coefficients, we assume that besides the SM contribution, only one of the NP operators in Eq. (3) is switched on at a time. We then compare the calculated ratios $R(D^{(*)})$ with the recent experimental data from the Belle, *BABAR*, and LHCb collaborations [1–5] given in Eq. (1). We also take into account a theoretical error of 10% for the ratios $R(D^{(*)})$.

The experimental constraints are shown in Fig. 2. The vector operators $\mathcal{O}_{V_{L,R}}$ and the left scalar operator \mathcal{O}_{S_L} are favored while there is no allowed region for the right scalar operator \mathcal{O}_{S_R} within 2σ . Therefore we will not consider \mathcal{O}_{S_R} in what follows. The tensor operator \mathcal{O}_{T_L} is less favored, but it can still well explain the current experimental results.

The stringent constraint on the tensor coupling mainly comes from the experimental data of $R(D^*)$.

In each allowed region at 2σ we find the best-fit value for each NP coupling. The best-fit couplings read

$$\begin{aligned} V_L &= -0.23 - i0.85, & V_R &= 0.03 + i0.60, \\ S_L &= -1.80 - i0.07, & T_L &= 0.38 + i0.06, \end{aligned} \tag{20}$$

and are marked with an asterisk. The allowed regions of the coupling coefficients are then used to analyze the effect of the NP operators on different physical observables defined in the next section.

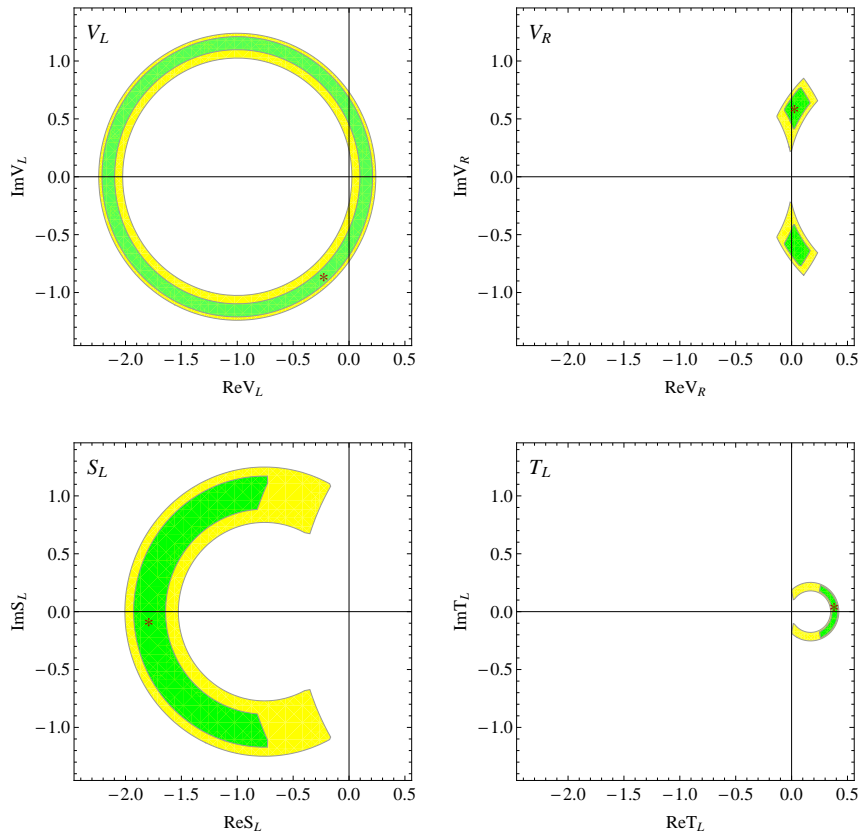


FIG. 2: The allowed regions of the Wilson coefficients $V_{L,R}$, S_L , and T_L within 1σ (green, dark) and 2σ (yellow, light). The best-fit value in each case is denoted with the symbol *. The coefficient S_R is disfavored at 2σ and therefore is not shown here.

IV. THE CASCADE DECAY $\bar{B}^0 \rightarrow D^{*+}(\rightarrow D^0\pi^+)\tau^-\bar{\nu}_\tau$ AND THE ANGULAR OBSERVABLES

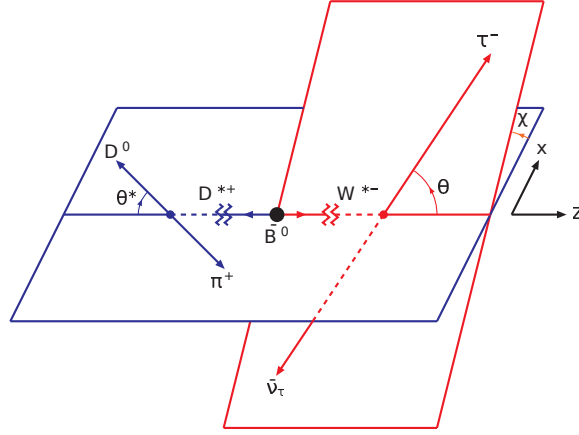


FIG. 3: Definition of the angles θ , θ^* and χ in the cascade decay $\bar{B}^0 \rightarrow D^{*+}(\rightarrow D^0\pi^+)\tau^-\bar{\nu}_\tau$. See text for more details.

A. The fourfold distribution

In order to analyze NP effects on the polarization of the D^* meson one uses the cascade decay $\bar{B}^0 \rightarrow D^{*+}(\rightarrow D^0\pi^+)\tau^-\bar{\nu}_\tau$. A detailed derivation of the fourfold angular distribution (without NP) can be found in our paper [52]. The three angles θ , θ^* , and χ in the distribution are defined in Fig. 3 [28, 35, 53]. Here, θ is the polar angle between the τ^- three-momentum and the direction opposite to the D^* meson in the W^- rest frame, and θ^* is the polar angle between the three-momentum of the final meson D^0 and the direction of the D^* meson in the $(D^0\pi^+)$ rest frame. The $\bar{B}^0 \rightarrow D^{*+}\tau^-\bar{\nu}_\tau$ decay plane is spanned by the three-momenta of τ^- and $\bar{\nu}_\tau$ while the $D^{*+} \rightarrow D^0\pi^+$ decay plane is spanned by the three-momenta of the mesons D^0 and π^+ . And finally, χ is the azimuthal angle between the two planes. We choose a right-handed xyz coordinate system in the W^- rest frame such that the z axis is opposite to the direction of the mesons \bar{B}^0 and D^* , and the three-momentum of τ^- lies in the (xz) plane.

One has [54]

$$\frac{d^4\Gamma(\bar{B}^0 \rightarrow D^{*+}(\rightarrow D^0\pi^+)\tau^-\bar{\nu}_\tau)}{dq^2 d \cos \theta d \chi d \cos \theta^*} = \frac{9}{8\pi} |N|^2 J(\theta, \theta^*, \chi), \quad (21)$$

where

$$|N|^2 = \frac{G_F^2 |V_{cb}|^2 |\mathbf{p}_2| q^2 v^2}{(2\pi)^3 12m_1^2} \mathcal{B}(D^* \rightarrow D\pi). \quad (22)$$

The full angular distribution $J(\theta, \theta^*, \chi)$ is written as

$$\begin{aligned} J(\theta, \theta^*, \chi) &= J_{1s} \sin^2 \theta^* + J_{1c} \cos^2 \theta^* + (J_{2s} \sin^2 \theta^* + J_{2c} \cos^2 \theta^*) \cos 2\theta \\ &\quad + J_3 \sin^2 \theta^* \sin^2 \theta \cos 2\chi + J_4 \sin 2\theta^* \sin 2\theta \cos \chi \\ &\quad + J_5 \sin 2\theta^* \sin \theta \cos \chi + (J_{6s} \sin^2 \theta^* + J_{6c} \cos^2 \theta^*) \cos \theta \\ &\quad + J_7 \sin 2\theta^* \sin \theta \sin \chi + J_8 \sin 2\theta^* \sin 2\theta \sin \chi + J_9 \sin^2 \theta^* \sin^2 \theta \sin 2\chi, \end{aligned} \quad (23)$$

where $J_{i(a)}$ ($i = 1, \dots, 9; a = s, c$) are the angular observables. Their explicit expressions in terms of helicity amplitudes and Wilson coefficients read

$$\begin{aligned}
4J_{1s} &= \frac{3+2\delta_\tau}{4}(|1+V_L|^2+|V_R|^2)(|H_{++}|^2+|H_{--}|^2)-(3+2\delta_\tau)\text{Re}V_R H_{++}H_{--} \\
&\quad -8\sqrt{2\delta_\tau}\text{Re}T_L(H_{++}H_T^+ + H_{--}H_T^-) + 4(1+6\delta_\tau)|T_L|^2(|H_T^+|^2+|H_T^-|^2), \\
4J_{1c} &= 2|S_R-S_L|^2|H_V^S|^2+4\sqrt{2\delta_\tau}\text{Re}(S_R-S_L)H_V^S H_{0t} \\
&\quad +(|1+V_L|^2+|V_R|^2-2\text{Re}V_R)\left[4\delta_\tau|H_{0t}|^2+(1+2\delta_\tau)|H_{00}|^2\right] \\
&\quad -16\sqrt{2\delta_\tau}\text{Re}T_L H_{00}H_T^0+16(1+2\delta_\tau)|T_L|^2|H_T^0|^2, \\
4J_{2s} &= \frac{1}{4}(1-2\delta_\tau)\left[(|1+V_L|^2+|V_R|^2)(|H_{++}|^2+|H_{--}|^2) \right. \\
&\quad \left. -4\text{Re}V_R H_{++}H_{--}-16|T_L|^2(|H_T^+|^2+|H_T^-|^2)\right], \\
4J_{2c} &= (1-2\delta_\tau)\left[-(|1+V_L|^2+|V_R|^2-2\text{Re}V_R)|H_{00}|^2+16|T_L|^2|H_T^0|^2\right], \\
4J_3 &= (1-2\delta_\tau)\left[-(|1+V_L|^2+|V_R|^2)H_{++}H_{--} \right. \\
&\quad \left. +\text{Re}V_R(|H_{++}|^2+|H_{--}|^2)+16|T_L|^2H_T^+H_T^-\right], \\
4J_4 &= \frac{1}{2}(1-2\delta_\tau)\left[(|1+V_L|^2+|V_R|^2-2\text{Re}V_R)H_{00}(H_{++}+H_{--}) \right. \\
&\quad \left. -16|T_L|^2H_T^0(H_T^++H_T^-)\right], \\
4J_5 &= (|1+V_L|^2-|V_R|^2)H_{00}(H_{--}-H_{++}) \\
&\quad +2\delta_\tau(|1+V_L|^2+|V_R|^2-2\text{Re}V_R)H_{t0}(H_{++}+H_{--}) \\
&\quad +\sqrt{2\delta_\tau}\text{Re}(S_R-S_L)H_V^S(H_{++}+H_{--}) \\
&\quad +4\sqrt{2\delta_\tau}\text{Re}T_L[H_T^0(H_{++}-H_{--})-H_T^-(H_{00}+H_{t0})-H_T^+(H_{t0}-H_{00})] \\
&\quad -32\delta_\tau|T_L|^2H_T^0(H_T^+-H_T^-), \\
4J_{6s} &= (|1+V_L|^2-|V_R|^2)(|H_{--}|^2-|H_{++}|^2) \\
&\quad +8\sqrt{2\delta_\tau}\text{Re}T_L(H_{++}H_T^+-H_{--}H_T^-)-32\delta_\tau|T_L|^2(|H_T^+|^2-|H_T^-|^2), \\
4J_{6c} &= -8\delta_\tau(|1+V_L|^2+|V_R|^2-2\text{Re}V_R)H_{t0}H_{00} \\
&\quad -4\sqrt{2\delta_\tau}\text{Re}(S_R-S_L)H_V^S H_{00}+16\sqrt{2\delta_\tau}\text{Re}T_L H_{t0}H_T^0, \\
4J_7 &= \sqrt{2\delta_\tau}\text{Im}(S_R-S_L)H_V^S(H_{++}-H_{--})-4\delta_\tau\text{Im}V_R H_{t0}(H_{++}-H_{--}) \\
&\quad +4\sqrt{2\delta_\tau}\text{Im}T_L[H_T^0(H_{++}+H_{--})-H_T^-(H_{t0}+H_{00})+H_T^+(H_{t0}-H_{00})], \\
4J_8 &= (1-2\delta_\tau)\text{Im}V_R H_{00}(H_{--}-H_{++}), \\
4J_9 &= (1-2\delta_\tau)\text{Im}V_R(|H_{++}|^2-|H_{--}|^2). \tag{24}
\end{aligned}$$

The results for the angular functions J_i in Eq. (24) agree with those of Ref. [28] except for a difference in the sign of J_8 , J_9 , and the first two terms of J_7 . However, we find agreement with the results of our previous paper [35] in the case of J_7 , J_8 , and J_9 . Note again that in this paper we do not consider interference terms between different NP operators. In our quark model all helicity amplitudes are real, which implies the vanishing of all terms proportional to $\sin \chi$ and $\sin 2\chi$, namely $J_{7,8,9}$, within the SM. This does not necessarily hold when considering complex NP Wilson coefficients, as can be seen in Eq. (24).

B. The q^2 distribution and the ratios of branching fractions $R(D^{(*)})$

The fourfold distribution allows one to define a large set of observables which can help probe NP in the decay. First, by integrating Eq. (21) over all angles one obtains

$$\frac{d\Gamma(\bar{B}^0 \rightarrow D^* \tau^- \bar{\nu}_\tau)}{dq^2} = |N|^2 J_{\text{tot}} = |N|^2 (J_L + J_T), \quad (25)$$

where J_L and J_T are the longitudinal and transverse polarization amplitudes of the D^* meson, given by

$$J_L = 3J_{1c} - J_{2c}, \quad J_T = 2(3J_{1s} - J_{2s}). \quad (26)$$

The decay rate in Eq. (25) is often normalized over the corresponding muon mode in order to dismiss the poorly known V_{cb} and to partially cancel uncertainties from the hadronic form factors. In Fig. 4 we present the q^2 dependence of the rate ratios

$$R_{D^{(*)}}(q^2) = \frac{d\Gamma(\bar{B}^0 \rightarrow D^{(*)} \tau^- \bar{\nu}_\tau)}{dq^2} \bigg/ \frac{d\Gamma(\bar{B}^0 \rightarrow D^{(*)} \mu^- \bar{\nu}_\mu)}{dq^2} \quad (27)$$

in different NP scenarios. It is interesting to note that unlike the vector and scalar operators, which tend to increase both ratios, the tensor operator can lead to a decrease of the ratio $R(D^*)$ for $q^2 \gtrsim 8 \text{ GeV}^2$. Moreover, while the ratio $R(D^*)$ is minimally sensitive to the scalar coupling S_L (in comparison with other couplings, i.e. $V_{L,R}$, T_L), the ratio $R(D)$ shows maximal sensitivity to S_L . These behaviors can help discriminate between different NP operators.

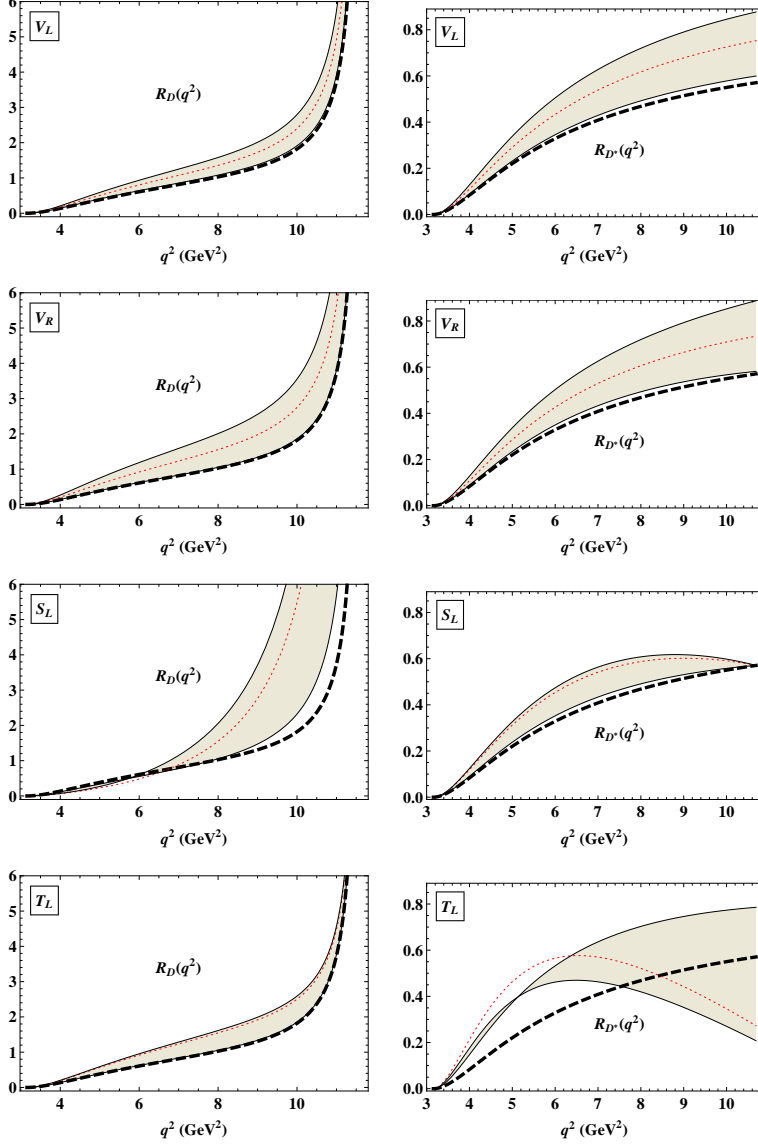


FIG. 4: Differential rate ratios $R_D(q^2)$ (left) and $R_{D^*}(q^2)$ (right). The thick black dashed lines are the SM prediction; the gray bands include NP effects corresponding to the 2σ allowed regions in Fig. 2; the red dotted lines represent the best-fit values of the NP couplings given in Eq. (20).

C. The $\cos\theta$ distribution, the forward-backward asymmetry, and the lepton-side convexity parameter

We define a normalized angular decay distribution $\tilde{J}(\theta^*, \theta, \chi)$ through

$$\tilde{J}(\theta^*, \theta, \chi) = \frac{9}{8\pi} \frac{J(\theta^*, \theta, \chi)}{J_{\text{tot}}}, \quad (28)$$

where $J_{\text{tot}} = 3J_{1c} + 6J_{1s} - J_{2c} - 2J_{2s}$. The normalized angular decay distribution $\tilde{J}(\theta^*, \theta, \chi)$ obviously integrates to 1 after $\cos\theta^*$, $\cos\theta$, and χ integration. By integrating Eq. (21) over $\cos\theta^*$ and χ one obtains the differential $\cos\theta$ distribution which is described by a tilted parabola. The normalized form of the parabola reads

$$\tilde{J}(\theta) = \frac{a + b \cos\theta + c \cos^2\theta}{2(a + c/3)}. \quad (29)$$

The linear coefficient $b/2(a + c/3)$ can be projected out by defining a forward-backward asymmetry given by

$$\mathcal{A}_{FB}(q^2) = \frac{\int_0^1 d \cos\theta \, d\Gamma/d \cos\theta - \int_{-1}^0 d \cos\theta \, d\Gamma/d \cos\theta}{\int_0^1 d \cos\theta \, d\Gamma/d \cos\theta + \int_{-1}^0 d \cos\theta \, d\Gamma/d \cos\theta} = \frac{b}{2(a + c/3)} = \frac{3}{2} \frac{J_{6c} + 2J_{6s}}{J_{\text{tot}}}. \quad (30)$$

The coefficient $c/2(a + c/3)$ of the quadratic contribution is obtained by taking the second derivative of $\tilde{J}(\theta)$. Accordingly, we define a convexity parameter by writing

$$C_F^\tau(q^2) = \frac{d^2 \tilde{J}(\theta)}{d(\cos\theta)^2} = \frac{c}{a + c/3} = \frac{6(J_{2c} + 2J_{2s})}{J_{\text{tot}}}. \quad (31)$$

When calculating the q^2 averages of the forward-backward asymmetry and the convexity parameter, one has to multiply the numerator and denominator of Eqs. (30) and (31) by the q^2 -dependent piece of the phase-space factor $C(q^2) = |\mathbf{p}_2|q^2v^2$. For example, the mean forward-backward asymmetry can then be calculated according to

$$\langle \mathcal{A}_{FB} \rangle = \frac{3}{2} \frac{\int dq^2 C(q^2) (J_{6c} + 2J_{6s})}{\int dq^2 C(q^2) J_{\text{tot}}}. \quad (32)$$

The q^2 dependence of the forward-backward asymmetry is shown in Fig. 5. The coupling V_L does not effect \mathcal{A}_{FB} in both decays since it stands before the SM operator and drops out in the definition of the observable. In the case of the $\bar{B}^0 \rightarrow D^*$ transition, the operators \mathcal{O}_{V_R} , \mathcal{O}_{S_L} , and \mathcal{O}_{T_L} behave mostly similarly: they tend to decrease the forward-backward asymmetry and shift the zero-crossing point to greater values than the SM one. However, the tensor operator can also increase the asymmetry in the high- q^2 region. In the case of the $\bar{B}^0 \rightarrow D$ transition, the operator \mathcal{O}_{V_R} does not affect \mathcal{A}_{FB} , the tensor operator \mathcal{O}_{T_L} tends to lower \mathcal{A}_{FB} , and the scalar operator \mathcal{O}_{S_L} thoroughly changes \mathcal{A}_{FB} : it can increase the forward-backward asymmetry by up to 200% and implies a zero-crossing point, which is impossible in the SM. This unique effect of \mathcal{O}_{S_L} would clearly distinguish it from the other NP operators.

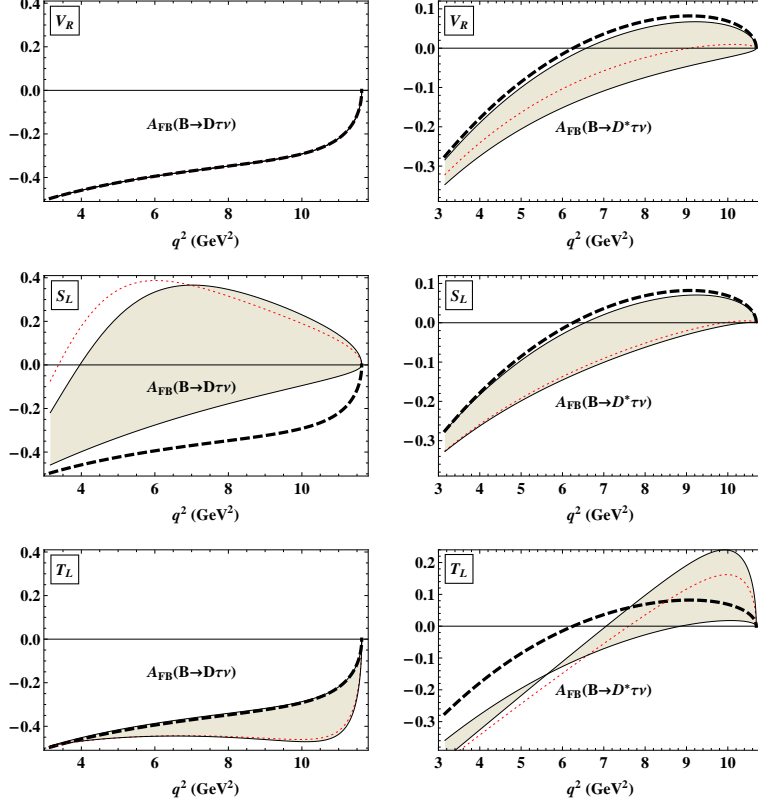


FIG. 5: Forward-backward asymmetry \mathcal{A}_{FB} for $\bar{B}^0 \rightarrow D\tau^-\bar{\nu}_\tau$ (left) and $\bar{B}^0 \rightarrow D^*\tau^-\bar{\nu}_\tau$ (right). Notations are the same as in Fig. 4.

In Fig. 6 we present the lepton-side convexity parameter $C_F^T(q^2)$. While $C_F^T(D)$ is only sensitive to \mathcal{O}_{TL} , $C_F^T(D^*)$ is sensitive to \mathcal{O}_{SL} , \mathcal{O}_{VR} , and \mathcal{O}_{TL} . Unlike \mathcal{O}_{SL} , which can only increase $C_F^T(D^*)$, the operator \mathcal{O}_{TL} can only lower the parameter. It is worth mentioning that $C_F^T(D)$ and $C_F^T(D^*)$ are extremely sensitive to \mathcal{O}_{TL} : it can change $C_F^T(D^{(*)})$ by a factor of 4 at $q^2 \approx 7 \text{ GeV}^2$.

D. The $\cos\theta^*$ distribution and the hadron-side convexity parameter

By integrating Eq. (21) over $\cos\theta$ and χ one obtains the hadron-side $\cos\theta^*$ distribution described by an untilted parabola (without a linear term). The normalized form of the $\cos\theta^*$ distribution reads $\tilde{J}(\theta^*) = (a' + c' \cos^2 \theta^*)/2(a' + c'/3)$, which can again be characterized by its convexity parameter given by

$$C_F^h(q^2) = \frac{d^2 \tilde{J}(\theta^*)}{d(\cos\theta^*)^2} = \frac{c'}{a' + c'/3} = \frac{3J_{1c} - J_{2c} - 3J_{1s} + J_{2s}}{J_{\text{tot}}/3}. \quad (33)$$

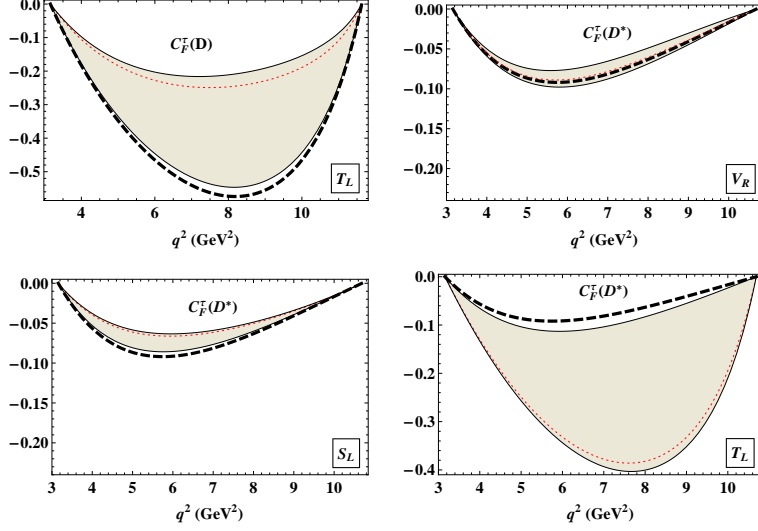


FIG. 6: Lepton-side convexity parameter $C_F^T(q^2)$. Notations are the same as in Fig. 4. In the case of the D meson, NP effects come from the tensor operator only.

The $\cos\theta^*$ distribution can be written as

$$\tilde{J}(\theta^*) = \frac{3}{4} (2F_L(q^2) \cos^2 \theta^* + F_T(q^2) \sin^2 \theta^*), \quad (34)$$

where $F_L(q^2)$ and $F_T(q^2)$ are the polarization fractions of the D^* meson and are defined as

$$F_L(q^2) = \frac{J_L}{J_L + J_T}, \quad F_T(q^2) = \frac{J_T}{J_L + J_T}, \quad F_L(q^2) + F_T(q^2) = 1. \quad (35)$$

The hadron-side convexity parameter and the polarization fractions of the D^* meson are related by

$$C_F^h(q^2) = \frac{3}{2} (2F_L(q^2) - F_T(q^2)) = \frac{3}{2} (3F_L(q^2) - 1). \quad (36)$$

The effects of NP operators on the hadron-side convexity parameter $C_F^h(q^2)$ are shown in

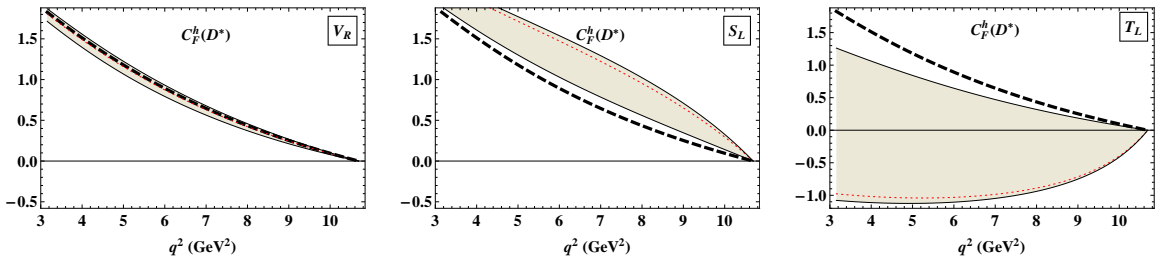


FIG. 7: Hadron-side convexity parameter $C_F^h(q^2)$. Notations are the same as in Fig. 4.

Fig. 7. Each NP operator can change $C_F^h(q^2)$ in a unique way: the vector operator \mathcal{O}_{V_R}

almost does nothing to the parameter; the scalar operator \mathcal{O}_{S_L} increases the parameter by about 50% nearly in the whole range of q^2 ; the tensor operator \mathcal{O}_{T_L} lowers the parameter (by up to 200% at low q^2), and it also allows negative values of $C_F^h(q^2)$, which are impossible in the SM.

E. The χ distribution and the trigonometric moments

By integrating Eq. (21) over $\cos\theta$ and $\cos\theta^*$ one obtains the χ distribution whose normalized form reads

$$\tilde{J}^{(I)}(\chi) = \frac{1}{2\pi} \left[1 + A_C^{(1)}(q^2) \cos 2\chi + A_T^{(1)}(q^2) \sin 2\chi \right], \quad (37)$$

where $A_C^{(1)}(q^2) = 4J_3/J_{\text{tot}}$ and $A_T^{(1)}(q^2) = 4J_9/J_{\text{tot}}$. Besides, one can also define other angular distributions in the angular variable χ as follows [27]:

$$J^{(II)}(\chi) = \left[\int_0^1 - \int_{-1}^0 \right] d\cos\theta^* \int_{-1}^1 d\cos\theta \frac{d^4\Gamma}{dq^2 d\cos\theta d\chi d\cos\theta^*}, \quad (38)$$

$$J^{(III)}(\chi) = \left[\int_0^1 - \int_{-1}^0 \right] d\cos\theta^* \left[\int_0^1 - \int_{-1}^0 \right] d\cos\theta \frac{d^4\Gamma}{dq^2 d\cos\theta d\chi d\cos\theta^*}. \quad (39)$$

The normalized forms of these distributions read

$$\tilde{J}^{(II)}(\chi) = \frac{1}{4} \left[A_C^{(2)}(q^2) \cos \chi + A_T^{(2)}(q^2) \sin \chi \right], \quad (40)$$

$$\tilde{J}^{(III)}(\chi) = \frac{2}{3\pi} \left[A_C^{(3)}(q^2) \cos \chi + A_T^{(3)}(q^2) \sin \chi \right], \quad (41)$$

where

$$A_C^{(2)}(q^2) = \frac{3J_5}{J_{\text{tot}}}, \quad A_T^{(2)}(q^2) = \frac{3J_7}{J_{\text{tot}}}, \quad A_C^{(3)}(q^2) = \frac{3J_4}{J_{\text{tot}}}, \quad A_T^{(3)}(q^2) = \frac{3J_8}{J_{\text{tot}}}. \quad (42)$$

Another method to project the coefficient functions J_i ($i = 3, 4, 5, 7, 8, 9$) out from the threefold angular decay distribution in Eq. (21) is to take the appropriate trigonometric moments of the normalized decay distribution $\tilde{J}(\theta^*, \theta, \chi)$ [35]. The trigonometric moments are defined by

$$W_i = \int d\cos\theta d\cos\theta^* d\chi M_i(\theta^*, \theta, \chi) \tilde{J}(\theta^*, \theta, \chi) \equiv \langle M_i(\theta^*, \theta, \chi) \rangle, \quad (43)$$

where $M_i(\theta^*, \theta, \chi)$ defines the trigonometric moment that is being taken. One finds

$$\begin{aligned}
W_T(q^2) &\equiv \langle \cos 2\chi \rangle = \frac{2J_3}{J_{\text{tot}}} = \frac{1}{2}A_C^{(1)}(q^2), \\
W_{IT}(q^2) &\equiv \langle \sin 2\chi \rangle = \frac{2J_9}{J_{\text{tot}}} = \frac{1}{2}A_T^{(1)}(q^2), \\
W_A(q^2) &\equiv \langle \sin \theta \cos \theta^* \cos \chi \rangle = \frac{3\pi}{8} \frac{J_5}{J_{\text{tot}}} = \frac{\pi}{8}A_C^{(2)}(q^2), \\
W_{IA}(q^2) &\equiv \langle \sin \theta \cos \theta^* \sin \chi \rangle = \frac{3\pi}{8} \frac{J_7}{J_{\text{tot}}} = \frac{\pi}{8}A_T^{(2)}(q^2), \\
W_I(q^2) &\equiv \langle \cos \theta \cos \theta^* \cos \chi \rangle = \frac{9\pi^2}{128} \frac{J_4}{J_{\text{tot}}} = \frac{3\pi^2}{128}A_C^{(3)}(q^2), \\
W_{II}(q^2) &\equiv \langle \cos \theta \cos \theta^* \sin \chi \rangle = \frac{9\pi^2}{128} \frac{J_8}{J_{\text{tot}}} = \frac{3\pi^2}{128}A_T^{(3)}(q^2).
\end{aligned} \tag{44}$$

These coefficient functions can also be projected out by taking piecewise sums and differences of different sectors of the angular phase space [55–58].

In Fig. 8 we show the q^2 dependence of the trigonometric moments $W_T(q^2)$, $W_I(q^2)$, $W_A(q^2)$, and $W_{IA}(q^2)$. The moments $W_T(q^2)$ and $W_I(q^2)$ are almost insensitive to \mathcal{O}_{V_R} but highly sensitive to \mathcal{O}_{T_L} . The scalar and tensor operators are likely to raise $W_T(q^2)$ and to lower $W_I(q^2)$ in general. The moment $W_A(q^2)$ shows great sensitivity to \mathcal{O}_{V_R} , \mathcal{O}_{S_L} , and \mathcal{O}_{T_L} . Both \mathcal{O}_{V_R} and \mathcal{O}_{T_L} tend to decrease $W_A(q^2)$ while \mathcal{O}_{S_L} tries to do the opposite. It is worth noting that all three moments $W_T(q^2)$, $W_I(q^2)$, and $W_A(q^2)$ are extremely sensitive to the tensor operator and their sign can change in the presence of \mathcal{O}_{T_L} . Regarding the moment $W_{IA}(q^2)$, the three operators act in the same manner: they can change the moment in both directions and the sensitivity is maximal in the case of \mathcal{O}_{V_R} .

The trigonometric moments $W_{II}(q^2)$ and $W_{IT}(q^2)$ are equal to zero in the SM and obtain a nonzero contribution only from the right-chiral vector operator \mathcal{O}_{V_R} , as depicted in Fig. 9. Both moments are proportional to the imaginary part of V_R and the effect of \mathcal{O}_{V_R} cancels in their ratio.

One can also consider certain combinations of angular observables where the form factor dependence drops out (at least in most NP scenarios), as described in Ref. [54]. As a demonstration, we consider the optimized observable

$$H_T^{(1)} = \frac{\sqrt{2}J_4}{\sqrt{-J_{2c}(2J_{2s} - J_3)}}, \tag{45}$$

which is equal to one not only in the SM but also in all NP scenarios except the tensor one, as shown in Fig. 10. Therefore $H_T^{(1)}(q^2)$ plays a prominent role in confirming the appearance

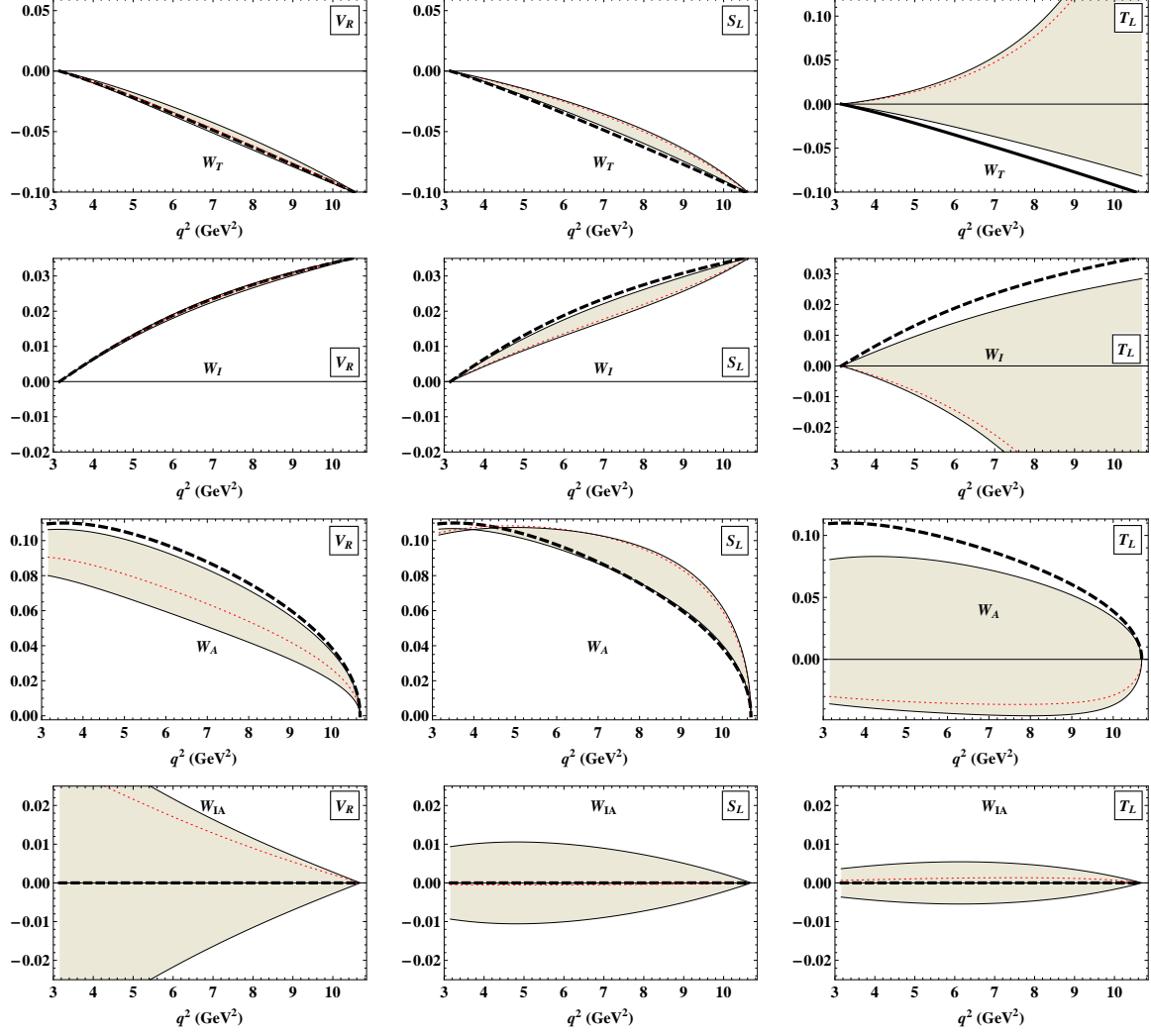


FIG. 8: Trigonometric moments $W_T(q^2)$, $W_I(q^2)$, $W_A(q^2)$, and $W_{IA}(q^2)$. Notations are the same as in Fig. 4.

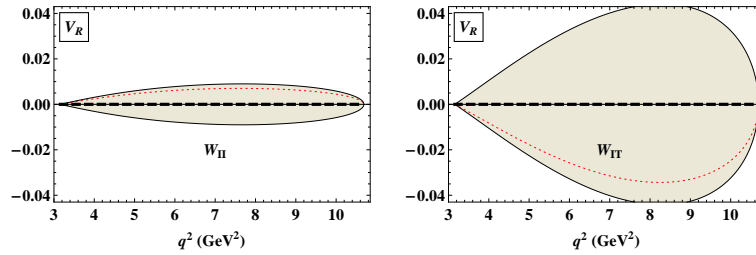


FIG. 9: Trigonometric moments $W_{II}(q^2)$ (left), and $W_{IT}(q^2)$ (right). Notations are the same as in Fig. 4.

of the tensor operator \mathcal{O}_{T_L} in the decay $\bar{B}^0 \rightarrow D^* \tau^- \bar{\nu}_\tau$.

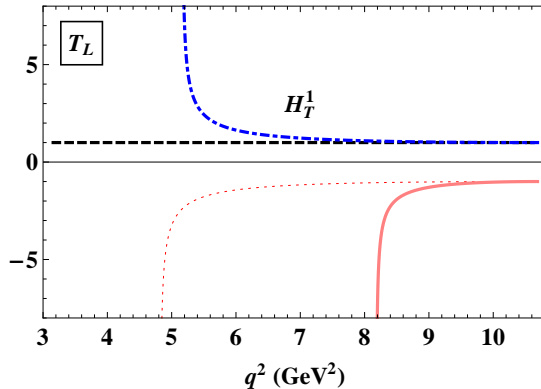


FIG. 10: Optimized angular observable $H_T^{(1)}(q^2)$ defined in Eq. (45). The black dashed line is the SM prediction. The red dotted line represents the best-fit value of T_L . The blue dot-dashed line and the pink solid line are the predictions for $T_L = 0.04 - 0.17i$ and $T_L = 0.18 + 0.23i$, respectively.

V. SUMMARY AND DISCUSSION

We have provided a thorough analysis of possible NP in the semileptonic decays $\bar{B}^0 \rightarrow D^{(*)} \tau^- \bar{\nu}_\tau$ using the form factors obtained from our covariant quark model. Starting with a general effective Hamiltonian including NP operators, we have derived the full angular distribution and defined a large set of physical observables which helps discriminate between NP scenarios. Assuming NP only affects leptons of the third generation and only one NP operator appears at a time, we have gained the allowed regions of NP couplings based on recent measurements at B factories and studied the effects of each operator on the observables. It has turned out that the current experimental data of $R(D)$ and $R(D^*)$ prefer the operators \mathcal{O}_{S_L} and $\mathcal{O}_{V_{L,R}}$, the operator \mathcal{O}_{T_L} is less favored, and the operator \mathcal{O}_{S_R} is disfavored at 2σ .

Our analysis has been done under the assumption of one-operator dominance. However, the large observable set has revealed unique behaviors of several observables and provided many correlations between them, which allows one to distinguish between NP operators. Our analysis can serve as a map for setting up various strategies to identify the origins of NP, one of which is as follows: first, one uses the null tests $W_{IT}(q^2) = 0$ and $H_T^{(1)}(q^2) - 1 = 0$ to probe the operators \mathcal{O}_{V_R} and \mathcal{O}_{T_L} , respectively. Second, one measures the forward-backward

asymmetry in the decay $\bar{B}^0 \rightarrow D\tau^-\bar{\nu}_\tau$. If $\mathcal{A}_{FB}^D(q^2)$ has a zero-crossing point, then it is a clear sign of the operator \mathcal{O}_{S_L} . The coupling V_L is more difficult to test because it is just a multiplier of the SM operator. However, if the tests above disconfirm \mathcal{O}_{V_R} , \mathcal{O}_{T_L} , and \mathcal{O}_{S_L} at the same time, then the modification of V_L to $R(D)$ and $R(D^*)$ is a must. In the future when more precise data will be collected, one can adopt the strategies described in this paper as a useful tool to discover NP in these decays if the deviation from the SM still remains.

Acknowledgments

The authors thank the Heisenberg-Landau Grant for providing support for their collaboration. M.A.I. acknowledges the support from PRISMA cluster of excellence (Mainz Uni.). M.A.I. and C.T.T. greatly appreciate warm hospitality of the Mainz Institute for Theoretical Physics (MITP) throughout their visit.

Appendix A: Relations for the form factors in the spectator quark model

The HQET relations for the form factors can be calculated using the formulas (see e.g., Ref. [59])

$$\begin{aligned}\langle D(p_2) | \bar{c}\Gamma b | \bar{B}(p_1) \rangle &= -\frac{1}{4\sqrt{m_1 m_2}} \text{tr}[(\not{p}_2 - m_2)\gamma_5 \Gamma (\not{p}_1 + m_1)\gamma_5] \cdot \xi(w), \\ \langle D^*(p_2) | \bar{c}\Gamma b | \bar{B}(p_1) \rangle &= -\frac{1}{4\sqrt{m_1 m_2}} \text{tr}[(\not{p}_2 - m_2)\epsilon_2^* \Gamma (\not{p}_1 + m_1)\gamma_5] \cdot \xi(w),\end{aligned}\quad (\text{A1})$$

where Γ denotes the Dirac operator that induces the transition,

$$w = \frac{2p_1 p_2}{2m_1 m_2} = \frac{m_1^2 + m_2^2 - q^2}{2m_1 m_2}, \quad q = p_1 - p_2,$$

and $\xi(w)$ is the universal Isgur-Wise function normalized to 1 at zero recoil $w = 1$. These relations allow one to express all form factors defined in Eqs. (6) and (7) in terms of the

Isgur-Wise function as

$$\begin{aligned}
F_{\pm}(q^2) &= \pm \frac{m_1 \pm m_2}{2\sqrt{m_1 m_2}} \cdot \xi(w), & F^S(q^2) &= \frac{\sqrt{m_1 m_2}}{m_1 + m_2} (w + 1) \cdot \xi(w), \\
F^T(q^2) &= \frac{m_1 + m_2}{2\sqrt{m_1 m_2}} \cdot \xi(w), \\
A_0(q^2) &= \frac{\sqrt{m_1 m_2}}{(m_1 - m_2)} (w + 1) \cdot \xi(w), \\
A_+(q^2) &= -A_-(q^2) = V(q^2) = \frac{m_1 + m_2}{2\sqrt{m_1 m_2}} \cdot \xi(w), \\
G_S(q^2) &= -\frac{m_2}{\sqrt{m_1 m_2}} \cdot \xi(w), & G_0^T(q^2) &= 0, \\
G_1^T(q^2) &= \frac{m_1 + m_2}{2\sqrt{m_1 m_2}} \cdot \xi(w), & G_2^T(q^2) &= -\frac{m_1 - m_2}{\sqrt{m_1 m_2}} \cdot \xi(w).
\end{aligned} \tag{A2}$$

One can use the equations of motion (EOMs) to obtain relations between the various form factors. The EOMs for the charm and the bottom fields read

$$\bar{\psi}_c \not{p}_c = m_c \bar{\psi}_c, \quad \not{p}_b \psi_b = m_b \psi_b. \tag{A3}$$

Using $p_1 - p_2 = p_b - p_c$ and the EOMs (A3) one can then relate the vector (axial) form factors to the scalar (pseudoscalar) form factors, and the tensor form factors to the vector (axial) form factors. One obtains

$$F_+(q^2)(m_1^2 - m_2^2) + F_-(q^2)q^2 = (m_b - m_c)(m_1 + m_2)F^S(q^2), \tag{A4}$$

$$-\frac{q^2}{(m_1 + m_2)}F^T = -(m_b + m_c)F_+ + (m_1 + m_2)F^S, \tag{A5}$$

$$\frac{(m_1^2 - m_2^2)}{(m_1 + m_2)}F^T = -(m_b + m_c)F_-, \tag{A6}$$

$$(m_b + m_c)G^S(q^2) = -(m_1 - m_2)A_0(q^2) + (m_1 - m_2)A_+(q^2) + \frac{q^2}{(m_1 + m_2)}A_-(q^2), \tag{A7}$$

$$(m_1^2 - m_2^2)G_1^T + q^2 G_2^T = +(m_b - m_c) \frac{(m_1^2 - m_2^2)}{m_1 + m_2} A_0, \tag{A8}$$

$$-G_1^T + \frac{q^2}{(m_1 + m_2)^2} G_0^T = -\frac{(m_b - m_c)}{m_1 + m_2} A_+ + G^S, \tag{A9}$$

$$-G_2^T - \frac{m_1^2 - m_2^2}{(m_1 + m_2)^2} G_0^T = +\frac{m_b - m_c}{(m_1 + m_2)} A_-. \tag{A10}$$

One can check that the HQET form factors satisfy the three relations Eqs. (A8), (A9), and (A10) for $m_b - m_c = m_1 - m_2$.

Appendix B: Heavy quark limit in the covariant quark model

In our approach the HQL was explored in great detail in Ref. [35] for the heavy-to-heavy transition $B \rightarrow D(D^*)$. It was explicitly shown that in the limit $m_B = m_b + E$, $m_b \rightarrow \infty$ and $m_D = m_{D^*} = m_c + E$, $m_c \rightarrow \infty$ we reproduce all relations given by Eqs. (A5), (A6), (A8), (A9), and (A10). In addition the Isgur-Wise function $\xi(w)$ has been calculated as follows:

$$\xi(w) = \frac{J_3(E, w)}{J_3(E, 1)}, \quad J_3(E, w) = \int_0^1 \frac{d\tau}{W} \int_0^\infty du \tilde{\Phi}^2(z) \left(\sigma_S(z) + \sqrt{\frac{u}{W}} \sigma_V(z) \right), \quad (\text{B1})$$

where $W = 1 + 2\tau(1 - \tau)(w - 1)$, $z = u - 2E\sqrt{u/W}$, and

$$\tilde{\Phi}(z) = \exp(-z/\Lambda^2), \quad \sigma_S(z) = \frac{m_u}{m_u^2 + z}, \quad \sigma_V(z) = \frac{1}{m_u^2 + z}.$$

It is readily seen that this function has the correct normalization at zero recoil, i.e. $\xi(w = 1) = 1$.

The subleading corrections to the heavy quark limit arising from finite quark masses have been investigated within our framework in Ref. [60]. In particular, it was found that the matrix element of the semileptonic decay $B \rightarrow D\ell\bar{\nu}$ calculated in the heavy quark limit up to the next-to-leading $1/m_Q$ order is written as

$$\begin{aligned} \langle D(p_2) | \bar{c}\gamma^\mu b | B(p_1) \rangle &= \sqrt{m_b m_c} \left\{ (v_1 + v_2)^\mu \left[\xi(w) + \left(\frac{1}{m_c} + \frac{1}{m_b} \right) \xi_+^{(1)}(w) \right] \right. \\ &\quad \left. + (v_1 - v_2)^\mu \left(\frac{1}{m_c} - \frac{1}{m_b} \right) \xi_-^{(1)}(w) \right\}, \end{aligned} \quad (\text{B2})$$

where the subleading function $\xi_+^{(1)}(w)$ is equal to zero at $w = 1$. Therefore, the subleading $1/m_Q$ corrections vanish at zero recoil $v_1 = v_2$ ($w = 1$) in accordance with Luke's theorem [61] (for review, see Ref. [31]).

One has to emphasize that HQL is just a great simplification of reality. In our approach hadrons are treated as bound states of quarks which are bound and confined. The matrix elements describing the transitions between hadrons are defined by the Feynman diagrams with virtual off-shell quarks. It is for this reason that the EOM relations are only approximately fulfilled in our model in the finite heavy quark mass case. The situation is rather different from the naive spectator quark model where quarks are supposed to be free and on shell. The calculation of the matrix elements in the CCQM is straightforward and does

not need to rely on either the EOM or the HQL. We mention that a discussion on decay constants and form factors in the $B \rightarrow D(D^*)$ transitions in the HQL can also be found in Ref. [62].

Appendix C: Twofold distribution of $\bar{B}^0 \rightarrow D^* \tau^- \bar{\nu}_\tau$

In this appendix we provide the explicit differential $(q^2, \cos \theta)$ distribution of the decay $\bar{B}^0 \rightarrow D^* \tau^- \bar{\nu}_\tau$ for easy comparison with other studies. The distribution reads

$$\begin{aligned}
& \frac{d^2\Gamma(\bar{B}^0 \rightarrow D^* \tau^- \bar{\nu}_\tau)}{dq^2 d\cos\theta} \\
&= \frac{G_F^2 |V_{cb}|^2 |\mathbf{p}_2| q^2 v^2}{32(2\pi)^3 m_1^2} \\
& \times \left\{ |1 + V_L|^2 \left[(1 - \cos\theta)^2 |H_{++}|^2 + (1 + \cos\theta)^2 |H_{--}|^2 + 2 \sin^2\theta |H_{00}|^2 \right. \right. \\
& \quad \left. \left. + 2\delta_\tau \left(\sin^2\theta (|H_{++}|^2 + |H_{--}|^2) + 2|H_{t0} - H_{00} \cos\theta|^2 \right) \right] \right. \\
& \quad \left. + |V_R|^2 \left[(1 - \cos\theta)^2 |H_{--}|^2 + (1 + \cos\theta)^2 |H_{++}|^2 + 2 \sin^2\theta |H_{00}|^2 \right. \right. \\
& \quad \left. \left. + 2\delta_\tau \left(\sin^2\theta (|H_{++}|^2 + |H_{--}|^2) + 2|H_{t0} - H_{00} \cos\theta|^2 \right) \right] \right. \\
& \quad \left. - 4\text{Re}V_R \left[(1 + \cos^2\theta) H_{++} H_{--} + \sin^2\theta |H_{00}|^2 \right. \right. \\
& \quad \left. \left. + 2\delta_\tau \left(\sin^2\theta H_{++} H_{--} + |H_{t0} - H_{00} \cos\theta|^2 \right) \right] \right. \\
& \quad \left. + 2|S_R - S_L|^2 |H_V^S|^2 \right. \\
& \quad \left. + 4\sqrt{2\delta_\tau} \text{Re}(S_R - S_L) H_V^S (H_{t0} - H_{00} \cos\theta) \right. \\
& \quad \left. + 16|T_L|^2 \left[|H_T^0|^2 \left(1 + 2\delta_\tau + (1 - 2\delta_\tau) \cos 2\theta \right) \right. \right. \\
& \quad \left. \left. + 2|H_T^+|^2 \sin^2 \frac{\theta}{2} \left(1 + 2\delta_\tau + (1 - 2\delta_\tau) \cos \theta \right) \right. \right. \\
& \quad \left. \left. + 2|H_T^-|^2 \cos^2 \frac{\theta}{2} \left(1 + 2\delta_\tau - (1 - 2\delta_\tau) \cos \theta \right) \right] \right. \\
& \quad \left. - 16\sqrt{2\delta_\tau} \text{Re}T_L \left[H_{++} H_T^+ + H_{--} H_T^- + H_{00} H_T^0 \right. \right. \\
& \quad \left. \left. - \left(H_{++} H_T^+ - H_{--} H_T^- + H_{t0} H_T^0 \right) \cos \theta \right] \right\}. \tag{C1}
\end{aligned}$$

-
- [1] J. Lees *et al.* (BABAR Collaboration), Phys. Rev. Lett. **109**, 101802 (2012), arXiv:1205.5442.
- [2] R. Aaij *et al.* (LHCb Collaboration), Phys. Rev. Lett. **115**, 111803 (2015) [Phys. Rev. Lett. **115**, 159901 (2015)], arXiv:1506.08614.
- [3] M. Huschle *et al.* (Belle Collaboration), Phys. Rev. D **92**, 072014 (2015), arXiv:1507.03233.
- [4] Y. Sato *et al.* (Belle Collaboration), Phys. Rev. D **94**, 072007 (2016), arXiv:1607.07923.
- [5] A. Abdesselam *et al.* (Belle Collaboration), arXiv:1608.06391.
- [6] H. Na *et al.* (HPQCD Collaboration), Phys. Rev. D **92**, 054510 (2015) Erratum: [Phys. Rev. D **93**, 119906 (2016)], arXiv:1505.03925.
- [7] S. Fajfer, J. F. Kamenik, and I. Nisandzic, Phys. Rev. D **85**, 094025 (2012), arXiv:1203.2654.
- [8] W. S. Hou, Phys. Rev. D **48**, 2342 (1993).
- [9] A. Crivellin, J. Heeck and P. Stoffer, Phys. Rev. Lett. **116**, 081801 (2016), arXiv:1507.07567.
- [10] A. Crivellin, C. Greub and A. Kokulu, Phys. Rev. D **86**, 054014 (2012), arXiv:1206.2634.
- [11] A. Celis, M. Jung, X. Q. Li and A. Pich, JHEP **1301**, 054 (2013), arXiv:1210.8443.
- [12] S. Nandi, S. K. Patra and A. Soni, arXiv:1605.07191.
- [13] S. P. Martin, Adv. Ser. Direct. High Energy Phys. **21**, 1 (2010), arXiv:hep-ph/9709356.
- [14] N. Deshpand and X. G. He, arXiv:1608.04817.
- [15] W. Buchmüller, R. Rückl, and D. Wyler, Phys. Lett. B **191**, 442 (1987).
- [16] L. Calibbi, A. Crivellin and T. Ota, Phys. Rev. Lett. **115**, 181801 (2015), arXiv:1506.02661.
- [17] Y. Sakaki, M. Tanaka, A. Tayduganov and R. Watanabe, Phys. Rev. D **88**, 094012 (2013), arXiv:1309.0301.
- [18] M. Bauer and M. Neubert, Phys. Rev. Lett. **116**, 141802 (2016), arXiv:1511.01900.
- [19] S. Fajfer and N. Kosnik, Phys. Lett. B **755**, 270 (2016), arXiv:1511.06024.
- [20] X. Q. Li, Y. D. Yang and X. Zhang, JHEP **1608**, 054 (2016), arXiv:1605.09308.
- [21] A. Greljo, G. Isidori and D. Marzocca, JHEP **1507**, 142 (2015), arXiv:1506.01705.
- [22] S. M. Boucenna, A. Celis, J. Fuentes-Martin, A. Vicente and J. Virto, Phys. Lett. B **760**, 214 (2016), arXiv:1604.03088.
- [23] A. Datta, M. Duraisamy, and D. Ghosh, Phys. Rev. D **86**, 034027 (2012), arXiv:1206.3760.
- [24] D. Becirevic, N. Kosnik, and A. Tayduganov, Phys. Lett. B **716**, 208 (2012), arXiv:1206.4977.
- [25] M. Tanaka and R. Watanabe, Phys. Rev. D **87**, 034028 (2013), arXiv:1212.1878.

- [26] P. Biancofiore, P. Colangelo, and F. De Fazio, *Phys. Rev. D* **87**, 074010 (2013), arXiv:1302.1042.
- [27] M. Duraisamy and A. Datta, *JHEP* **1309**, 059 (2013), arXiv:1302.7031.
- [28] M. Duraisamy, P. Sharma and A. Datta, *Phys. Rev. D* **90**, 074013 (2014), arXiv:1405.3719.
- [29] S. Bhattacharya, S. Nandi and S. K. Patra, *Phys. Rev. D* **93**, 034011 (2016), arXiv:1509.07259.
- [30] A. K. Alok, D. Kumar, S. Kumbhakar and S. U. Sankar, arXiv:1606.03164.
- [31] M. Neubert, *Phys. Rep.* **245**, 259 (1994), arXiv:hep-ph/9306320.
- [32] A. G. Grozin, *Heavy quark effective theory*, 201 (Springer Science & Business Media, 2014).
- [33] M. A. Ivanov, J. G. Körner, S. G. Kovalenko, P. Santorelli, and G. G. Saidullaeva, *Phys. Rev. D* **85**, 034004 (2012), arXiv:1112.3536.
- [34] T. Branz, A. Faessler, T. Gutsche, M. A. Ivanov, J. G. Körner and V. E. Lyubovitskij, *Phys. Rev. D* **81**, 034010 (2010), arXiv:0912.3710.
- [35] M. A. Ivanov, J. G. Körner and C. T. Tran, *Phys. Rev. D* **92**, 114022 (2015), arXiv:1508.02678.
- [36] G. V. Efimov and M. A. Ivanov, *Int. J. Mod. Phys. A* **4**, 2031 (1989).
- [37] G. V. Efimov and M. A. Ivanov, *The Quark Confinement Model Of Hadrons*, (CRC Press, 1993).
- [38] T. Gutsche, M. A. Ivanov, J. G. Körner, V. E. Lyubovitskij and P. Santorelli, *Phys. Rev. D* **88**, 114018 (2013), arXiv:1309.7879.
- [39] T. Gutsche, M. A. Ivanov, J. G. Körner, V. E. Lyubovitskij and P. Santorelli, *Phys. Rev. D* **86**, 074013 (2012), arXiv:1207.7052.
- [40] S. Dubnicka, A. Z. Dubnickova, M. A. Ivanov, J. G. Körner and G. G. Saidullaeva, *AIP Conf. Proc.* **1343**, 385 (2011), arXiv:1011.4417.
- [41] M. A. Ivanov and C. T. Tran, *Phys. Rev. D* **92**, 074030 (2015).
- [42] A. Salam, *Nuovo Cimento* **25**, 224 (1962); S. Weinberg, *Phys. Rev.* **130**, 776 (1963); K. Hayashi, M. Hirayama, T. Muta, N. Seto, and T. Shirafuji, *Fortschr. Phys.* **15**, 625 (1967).
- [43] C. Y. Cheung and C. W. Hwang, *JHEP* **1404** (2014) 177, arXiv:1401.3917.
- [44] C. Anastasiou, E. W. N. Glover and C. Oleari, *Nucl. Phys.* **B575**, 416 (2000); *Nucl. Phys.* **B585**, 763(E) (2000), arXiv: hep-ph/9912251.
- [45] M. Re Fiorentin, *Int. J. Mod. Phys. C* **27**, 1650027 (2015), arXiv:1507.03527.
- [46] T. Gutsche, M. A. Ivanov, J. G. Körner, V. E. Lyubovitskij, P. Santorelli and N. Haby, *Phys. Rev. D* **91**, 074001 (2015); *Phys. Rev. D* **91**, 119907(E) (2015), arXiv:1502.04864.

- [47] G. Ganbold, T. Gutsche, M. A. Ivanov and V. E. Lyubovitskij, *J. Phys. G* **42**, 075002 (2015), arXiv:1410.3741.
- [48] A. Issadykov, M. A. Ivanov and S. K. Sakhiyev, *Phys. Rev. D* **91**, 074007 (2015), arXiv:1502.05280.
- [49] K. A. Olive *et al.* (Particle Data Group), Review of particle physics, *Chin. Phys. C* **38**, 090001 (2014).
- [50] J. F. Kamenik and F. Mescia, *Phys. Rev. D* **78**, 014003 (2008), arXiv:0802.3790.
- [51] J. A. Bailey *et al.* (MILC Collaboration), *Phys. Rev. D* **92**, 034506 (2015), arXiv:1503.07237.
- [52] A. Faessler, T. Gutsche, M. A. Ivanov, J. G. Körner and V. E. Lyubovitskij, *Eur. Phys. J. direct C* **4**, 18 (2002), arXiv:hep-ph/0205287.
- [53] X. W. Kang, B. Kubis, C. Hanhart and U. G. Meiner, *Phys. Rev. D* **89**, 053015 (2014), arXiv:1312.1193.
- [54] T. Feldmann, B. Müller and D. van Dyk, *Phys. Rev. D* **92**, 034013 (2015), arXiv:1503.09063.
- [55] J. G. Körner and G. A. Schuler, *Phys. Lett. B* **231**, 306 (1989).
- [56] J. G. Körner and G. A. Schuler, *Z. Phys. C* **46**, 93 (1990).
- [57] J. Gratex, M. Hopfer and R. Zwicky, *Phys. Rev. D* **93**, 054008 (2016), arXiv:1506.03970.
- [58] D. Becirevic, S. Fajfer, I. Nisandzic and A. Tayduganov, arXiv:1602.03030.
- [59] J. G. Körner and G. A. Schuler, *Z. Phys. C* **38**, 511 (1988); *Z. Phys. C* **41**,690(E) (1989).
- [60] M. A. Ivanov, O. E. Khomutenko and T. Mizutani, *Phys. Rev. D* **46**, 3817 (1992).
- [61] M. E. Luke, *Phys. Lett. B* **252**, 447 (1990).
- [62] M. De Vito and P. Santorelli, *Eur. Phys. J. C* **40**, 193 (2005), arXiv:hep-ph/0412388.